Electrically Conductive Gold-Coated Collagen Nanofibers for Placental-Derived Mesenchymal Stem Cells Enhanced Differentiation and Proliferation

Anamaria Orza,[†,*] Olga Soritau,[‡] Liliana Olenic,[§] Mircea Diudea,[†] Adrian Florea,[⊥] Dan Rus Ciuca,[⊥] Carmen Mihu,[⊥] Daniel Casciano,[∥] and Alexandru S. Biris[∥,*]

[†]Faculty of Chemistry and Chemical Engineering, Babes-Bolyai University, Cluj-Napoca, Romania, [‡]The Oncology Institute Prof. Dr. Ion Chiricuta, Cluj-Napoca, Romania, [§]National Institute for Research and Development of Isotopic and Molecular Technologies, Cluj-Napoca, Romania, [⊥]"Iuliu Hatieganu" University of Medicine and Pharmacy, Cluj-Napoca, Romania, and [∥]Nanotechnology Center, University of Arkansas at Little Rock, Little Rock, Arkansas 72204, United States

ABSTRACT Gold-coated collagen nanofibers (GCNFs) were produced by a single-step reduction process and used for the growth and differentiation of human adult stem cells. The nanomaterials were characterized by a number of analytical techniques including electron microscopy and spectroscopy. They were found to be biocompatible and to improve the myocardial and neuronal differentiation process of the mesenchymal stem cells isolated from the placental chorionic component. The expression of specific differentiation markers (atrium, natriuretic peptide, actin F and actin monomer, glial fibrilary acidic protein, and neurofilaments) was investigated by immunocytochemistry.

KEYWORDS: collagen · gold-coated collagen fibers · stem cell differentiation and proliferation

There is considerable interest in synthesizing 1-, 2-, and 3-D nano structures with novel physical and chemical properties since such complex materials present great potential for fundamental and practical research in the fields of biology and regenerative medicine.[1] New advances in these areas are provided by the use of nanostructured materials that, given their unique electronic, optical, magnetic, and structural properties, are ideal to study and to explore biological systems at the molecular and cellular levels.[2]

A variety of engineered nanostructures have been produced by the specific attachment between an inorganic compound and an organic surfactant,[3,4] polymer,[5] or biological molecule (DNA, peptides, or proteins). Recently, hybrid inorganic/organic materials have been synthesized by using DNA or viruses as scaffolds.[6,7] Some proteins and peptides are excellent scaffolds[8,9] for tissue regeneration because of their chemical structural diversity (aliphatic, acidic, basic, or aromatic side chains) and their large number of architectures (helices, β-sheets, and tubules).[10−12] A new emphasis in regenerative medicine is to use multifunctional and biologically active scaffolds to study differentiation and proliferation of stem cells on such surfaces. As a result, three factors are seen as being essential for a successful tissue-engineering platform: (1) the differentiation and proliferation potential of various types of stem cells; (2) scaffolds that sustain the cells at high proliferation and differentiation; and (3) the use of specific growth and differentiation factors.[13]

Stem cells are characterized by their self-renewal ability and differentiation potential and can be divided into embryonic and adult stem cells. Mesenchymal stem cells (MSCs) are minor populations of adult stem cells found in adult organs with similar phenotypic characteristics that have the capacity to be expanded *ex vivo* and stimulated to proliferate and differentiate when they are exposed to growth factors in tissue culture. Numerous reports demonstrate the MSCs' ability to differentiate into several lineages, including osteocytes, chondrocytes, myocytes, adipocytes, cardiomyocytes—and even into cells of nonmesodermal origin, including hepatocytes, insulin-producing cells, and neurons.[14−16] Placental-derived MSC cells have several major advantages: they are multipotent (they can differentiate into all three germ layers) and have low immunogenicity and

* Address correspondence to iorza@chem.ubbcluj.ro, asbiris@ualr.edu.

Received for review December 20, 2010 and accepted May 24, 2011.

Published online May 24, 2011
10.1021/nn1035312

anti-inflammatory functions.[17] The immunosuppressive properties of placental-derived MSCs are explained by the fact that they do not express HLA-DR molecules.[18] As a result, these stem cells have the potential to play a major role in tissue regeneration, replacing nonfunctional tissues lost during various diseases or accidents. This is especially true after heart failure due to myocardial infarction that results in the loss of cardiomyocytes combined with the absence of endogenous repair mechanisms.

Human mesenchymal stem cells (hMSCs) differentiate into various cell lineages, but only a small percentage of the cells used for transplantation will actually differentiate into cardiomyocytes when they are implanted into a patient. As a result, the efficiency of differentiation that will actually control the overall success and efficacy of the treatment could be significantly enhanced if the undifferentiated cells were directed *in vitro* prior to development into cardiomyogenic or neuronal lineages.[19] Some studies have demonstrated that exogenous cells can engraft in adult myocardium and, in some cases, have a measurable functional impact on the damaged myocardium.[20] Regeneration of damaged cardiomyocytes and other cell types, such as neurons, requires a mechanically stable implant material to support cellular proliferation and development.

Multifunctional and multicomponent biodegradable and nonbiodegradable scaffolds present a promising solution for cellular support, given their flexible properties such as mechanical strength, biocompatibility, and chemical inertness. Thus, there is a need to explore the possibility of employing various materials for functional cellular regeneration, which can present complex challenges.[16,21] A variety of natural biomaterials such as laminin, fibronectin, and collagen are typically employed to improve the efficacy of substrates used in tissue reconstruction. However, these materials induce undesirable immune responses when implanted into living organisms, and they lack mechanical stability and strength. Biomaterials built at the nanoscale could possess the desired surface bioactivity and porosity required for a successful tissue-engineering platform that employs hMSC. However, concerns still exist regarding the cytotoxicity of nanomaterials when introduced into tissues or exposed to cells. The biological effects of some nanoparticles have already been assessed for uptake and distribution within stem cells, their influence on stem cell viability, proliferation, differentiation, and cytotoxicity.[22] Among all of the nanomaterials, some of the most intensively studied are gold nanoparticles (GNPs) because of their high biocompatibility and easy functionalization with biomolecules, that is, growth factors, DNA, peptides, *etc*. GNPs have been successfully used as drug delivery systems and therapeutic agents and as thermal agents in cancer photothermal/photoacoustic therapy.[23]

One of the most commonly used biomaterials in tissue engineering is collagen; it is biocompatible and has excellent rates of biointegration and biodegradability. Additionally, its properties can be improved by several cross-linking procedures—including reactions with glutaraldehyde, isocyanates, epoxides, and bisimidates, as well as thermal treatment, UV or γ-ray irradiation, and photo-oxidation. By using GNPs as a cross-linking agent in collagen gels, different biomolecules such as growth factors, cell adhesion molecules, and peptides are easily incorporated through their biochemical immobilization at the gold surface without additional alteration of the collagen structure.[24] At present, very little is known about the behavior of stem cell proliferation capabilities on nanostructural biomaterials or on gold fibrous interfaces.[25] Gold-coated collagen fibers formed into film substrates (MC) are promising building blocks for the construction of a new generation of flexible substrates having a high capacity to sustain cell differentiation and to allow accurate drug and DNA plasmid delivery, which are often required for the successful development of multifunctional scaffolds for tissue engineering. Here, we report for the first time, to the best of our knowledge, the preparation of such multicomponent nanostructural coatings and their induced effects on placental-derived mesenchymal stem cell differentiation into myocardial and neuronal cells. The major goal of this study was to show that the gold-coated collagen fibers (GCNFs) are excellent materials for the enhanced proliferation and differentiation of the MSC. Such technologies could be the foundation for technological platforms for the regeneration of nerves, bone, skin, and other tissues in a controllable and practical manner.

RESULTS AND DISCUSSION

Gold-Coated Collagen Substrates (MC) and Their Corresponding Chemical and Physical Properties. Gold-coated collagen substrates were prepared by using a layer-by-layer method, where each layer is the foundation for the subsequent layer, and were composed of homogeneous gold-coated collagen nanofibers, GCNFs. Such nanofiber formation has not been intensively studied so far. Most investigations have reported the cross-linking between collagen molecules and gold nanoparticles.[26] Our work includes the assembly of nanofibers of various lengths—both with and without reducing agents—and under variable pH conditions. Our original approach for the synthesis of variable length gold metal-coated collagen fibers (from short to medium and long nanofibers, within a pH range of 3.5−11 using sodium citrate/borohydrate as reducing agents or without any reducing agent) was as follows: in the first stage, collagen was mixed with tetrachloroauric acid in a molar ratio 1:1. Gold ions interact either electrostatically, forming weak hydrogen bonds, or

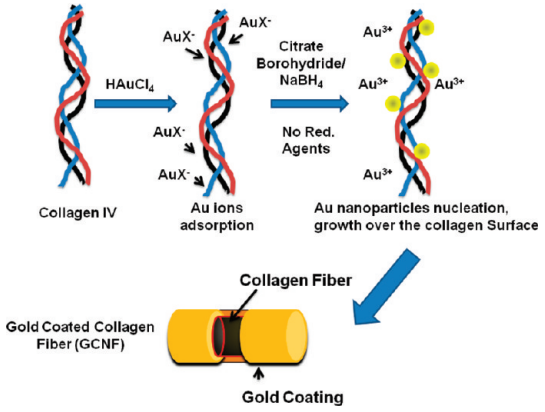

Figure 1. Schematic for the collagen gold coating process, resulting in collagen nanofibers coated with thin layers of gold (GCNF).

chemically, forming weak covalent bonds with collagen through amide functional groups.[27] In the second stage, citrate-reducing agent or $NaBH_4$ was added to the solution, and $HAuX^-$ ions (X = OH or Cl) were transformed onto metallic film nanostructures. The metallization process of collagen used and developed during this study is presented in Figure 1. A change of color occurred, and the solution turned from transparent to pink. When no reducing agent was added, Au(III) was reduced to Au(0) by the functional groups that have reduction capabilities and are present on the collagen surface. This process occurred only in acidic medium. The pH of the solution influences the nucleation and growth of Au crystals on the collagen substrate. Recently, GNPs of various sizes have been synthesized by the reduction of $HAuCl^-$ ions on the substrate by different kinds of reducing agents at various pH ranges.[28]

By using the above-mentioned method, we successfully generated GCNFs with various lengths by the simple manipulation of the assembly conditions. Increasing the pH from 3.5 to 11 and decreasing the speed of mixing resulted in molecular aggregates that have the ability to link end-to-end to create different nanofiber lengths and diameters. Short nanofibers, having a homogeneous sedimentation, were produced with $HAuCl_4$/collagen/sodium citrate ratio of 1:1:1 (w/w) at pH = 3.5 by mixing the solution at high speed to increase turbulence and exposure (Figure 2Aa). Under the same conditions but with increasing pH (pH = 5.5−6.5), the collagen molecules form more highly ordered structures, as presented in Figure 2Ab,c. Under neutral and slightly alkaline conditions (pH 7.0−9.0), we obtained longer nanofibers but with a nonhomogenous surface gold coating distribution (Figure 2Ad,e). In more alkaline medium, slightly distorted nanofibers were obtained (Figure 2f). Nanofibers formed by using $NaBH_4$ (Figure 2Ag,h) as the reducing agent have almost the same length (1.2−1.8 μm) as in the case of sodium citrate (Figure 2Ab,c), but they differ in diameter: width = 60−65 nm for citrate and 20−27 nm for borohydride. In the absence of a reducing agent and acidic pH = 5.5, long metallized nanofibers (length = 1−2 μm, width = 30−35 nm) formed (Figure 2Ai). The adsorption is higher in the acidic region (pH 3.5−5.5), indicating that slightly acidic conditions favor the reduction of Au(III) ions. During the adsorption of gold nanoparticles onto the collagen surface, several interactions—such as electrostatic attraction, covalent or hydrogen bonds—occur. Limited data are available that describe the precise location of the binding sites in the chemisorption process of colloidal gold or ions onto the collagen surface.[29]

Variable lengths of collagen nanofibers were produced by a single-step reduction process, and they were assembled layer-by-layer in order to form a high property gold metal-coated collagen substrate. UV−vis and FTIR spectroscopy, transmission electron microscopy (TEM), and conductivity measurements were used to characterize the substrate.

UV−vis spectroscopy confirmed the formation and adsorption of gold ions over the surface of the collagen macromolecules; this process was monitored after 30 min and 24 h, respectively (Supporting Information Figure 1). UV−vis spectroscopy is an excellent method for studying GCNF formation and their agglomeration. During aggregation, the shifting and broadening of surface plasmonic bands were observed to occur. Rarely, a second adsorption shoulder is observed due to self-assembly of nanoparticles[30] into linear nanostructures. Here, the nanofiber solution shows broad adsorption bands at around 300 nm and adsorption peaks centering between 520 and 540 nm. This adsorption peak is characteristic of gold metal nanostructures,[31] and its intensity increases with time, indicating the formation of nanostructures attached to collagen. The broad absorption bands around 300 nm suggest the existence of $HAuCl_4$ in solution. Comparing cases a and b (Supporting Information Figure 1), it can be concluded that, when the reducing agent is added, nucleation and growth occur more quickly; the nanoparticles are more homogenously distributed, and no agglomeration is observed. In the case presented in Figure 1B in the Supporting Information, with no reduction agent used, the reduction occurs in time, and the broad peak around 520−540 nm suggests that the particles tend to agglomerate.

The interaction between gold nanoparticles and collagen macromolecules indicated by TEM and UV−vis spectroscopy was also confirmed by FTIR analysis, as shown in Figure 2B. Some FTIR characteristic peaks for pure collagen were found to have changed their positions, while others disappeared when GNPs were attached to the collagen structure. The upper region at 3750−2750 cm^{-1} changed dramatically. The C−H stretching corresponding peaks

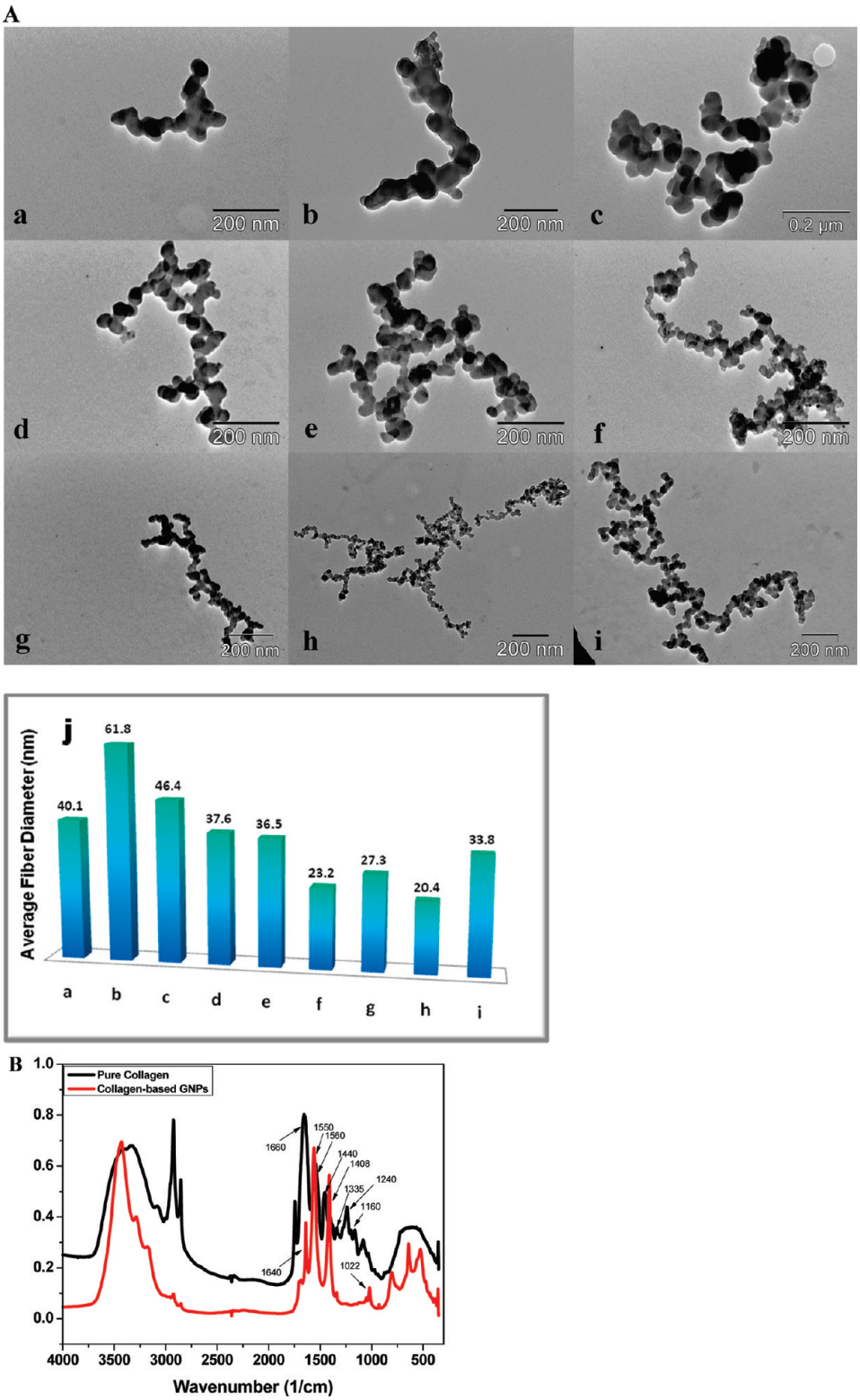

Figure 2. (A) Transmission electron microscopy (TEM) images along with the histogram of the size distribution of collagen-based gold nanofibers. TEM images of collagen-based gold nanoparticles with and without reducing agent at different pH: (a) sodium citrate short nanofibers at pH = 3.5; (b) medium nanofibers pH = 5.5; longer nanofibers at (c) pH = 6.5, (d) pH = 7, (e) pH = 9, (f) pH = 11. No reducing agent: $NaBH_4$ long nanowires at pH = 5.5 (g) and longer nanowires at pH = 7 (h); (j) representative histogram of gold nanofibers obtained under different conditions. (B) FTIR spectra of collagen and GCNF produced at pH = 5.5 (panel Ab).

from 2700 to 3000 cm^{-1} disappeared, and the single band at 3375 cm^{-1} arose after metal absorption. This band is given by the stretching vibrations of the NH^{3+} groups that are involved in electrostatic bonds with

gold. Moreover, the absence of C—H stretching bands, in contrast with their presence in pure collagen, is due to the chain length of collagen and its molecules' parallel orientation on the gold surface. The molecules pack to densities sufficient to form high-quality barriers for both electron- and ion-transfer processes.[32] Furthermore, the amide I absorption, characteristic of C═O stretching vibrations, appears with a position changed from 1660 to 1640 cm^{-1}; amide II absorption, N—H bending vibrations, and C—N stretching vibrations shifted from 1550 to 1560 cm^{-1}; amide III, C—N stretching, and N—H in plane bending shifted from 1240 to 1022 cm^{-1} because of their interactions with the GCNF surfaces. Also, the characteristic vibrations of the COO^- groups or C—O vibrations of alcohols from the hydroxyprolyne or glycosidic side chain shifted from 1440 to 1408 cm^{-1}. In this case, the peak intensities dramatically decreased along with band broadening.

To demonstrate their potential applications as an electrically conductive substrate for placental-derived mesenchymal stem cell differentiation, we investigated their electrical properties by using *I*—*V* measurements. The continuous coverage of the collagen fibers with gold metal particles shown by transmission electron microscopy suggests that they are electrically conductive. The current—voltage (*I*—*V*) curves of the gold metal-coated collagen substrate with its measured electrical resistance value of 2.36 MΩ are presented in Figure 2 in the Supporting Information. The *I*—*V* sweeps (cycles 1 and 2) do not present a typical ohmic character, but instead present symmetric current plateaus centered upon zero voltage, indicative of electron-tunneling barriers. Because the nanofibers were generated by chemical reaction, there are many grain boundaries that hinder the current flow. This behavior is not surprising, and the electron conduction takes place through hopping between the adjacent domains.[33] Repetitive cycling of the device could reduce these effects until almost purely ohmic behavior is obtained. In our case, after 15 cycles of *I*—*V* scans, an ohmic behavior with a resistivity value estimated to be 4×10^{-5} Ωm was measured. It is believed that this cycling process anneals the metal grains and improves the current transport through the substrate.

Regenerative medicine demands an ideal scaffold for stem cell differentiation that should offer adhesive moieties incorporated into biomaterials, expressed in a spatial and temporal manner to control cellular behaviors and mediate specific receptor—ligand interactions.[34] Moreover, cell and nuclear targeting are often necessary, and this could be affected by different nanostructures.[35] Gold nanoparticles are convenient due to their nontoxic and antiseptic properties and their rapid intracellular uptake *via* an endolysosomal path dependent upon the size and shape of the nanostructure.[36] Our motivation for this study was to examine the growth and differentiation of human placental-derived mesenchymal stem cells exposed to differentiation media and when grown on collagen as control and gold metal-coated collagen with and without electrical stimulation. As shown by the TEM analysis, the gold-coated collagen fibers prepared at a pH of 5.5 (Figure 2Ab) had the most uniform morphologies and significant gold coating (larger diameter); as a result, we have subsequently used them for all cellular proliferation and differentiation studies.

Gold-Coated Collagen Substrate (MC) Effects on the Growth and Differentiation of Human Placental-Derived Mesenchymal Stem Cells. The extracellular matrix and its most abundant component, collagen, have the capacity to regulate multiple functions of diverse cell types. Placental-derived MSCs have a high response to matrix components, such as collagen, laminin, or a combination of collagen and laminin, most probably by a mechanotransduction signal through integrin molecules. For their differentiation into cardiac and neuronal cells, a solid substrate with specific morphological, mechanical, and electrical properties is needed as the extracellular matrix to develop their characteristic functions. The nanoscale spatial organization of collagen fibrils is believed to be crucial for neurite guidance in neural development and repair, as well as for cardiomyocyte development.[37]

Rowlands *et al.* have shown that there is significant interplay between the particular matrix structure, such as collagen IV and laminin I, exposed to the MSCs and the underlying substrate elasticity that affects myogenic or osteogenic differentiation.[38] In another study, Suzuki *et al.* cultured MSCs on Petri dishes coated with three types of extracellular matrix components (ECM) including laminin, collagen type IV, and fibronectin for 7 days and demonstrated an increased proliferation of MSCs on collagen IV-coated dishes. They also found a significant up-regulation of smooth muscle cell genes and proteins on laminin-coated dishes.[39]

On the basis of these considerations, we examined the ability of placental-derived MSCs to differentiate into cardiomyocyte and neuronal lineages when cultivated *in vitro* on different substrates, for example, none (ctrl), collagen only (coll), and metal-coated collagen nanofibers (GCNF) substrates noted as MC. The metal-absorbed collagen substrates proved to be the most effective. Moreover, we demonstrated that the spatial arrangement of collagen along with the potential of GCNFs to deliver electrical stimulation induces a faster neuronal and cardiac differentiation of the stem cells when the metal-absorbed collagen substrate is exposed to electrical stimulation.

When cells were cultured over the MC substrates, few of the substrate fibers were observed to be internalized during the first few hours. Recent literature[40] has shown that MSCs have the capacity to bind and uptake collagen through their uPAR-associated

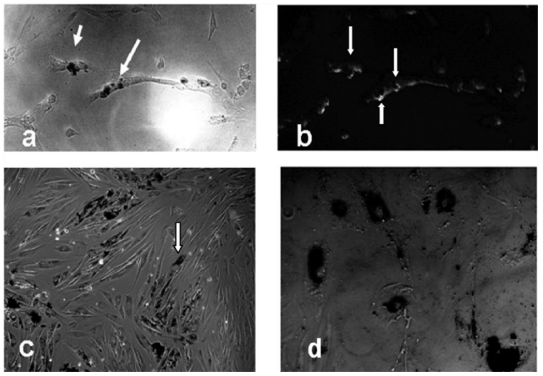

Figure 3. Chorion-derived MSC cultivated on gold-coated collagen (GCNF) substrate (MC) showing intracellular intake of the metallized fibers; 3 days of cultivation phase contrast image (a) and dark field image (b) (magnification 200×); 13 days of cultivation in the presence of myocardial differentiation medium and after (c) 1 month of cultivation with neuronal differentiation medium; (d) phase contrast image magnification 400×.

proteins uPARAP/Endo180, with the FnII domain being responsible for the binding and uptake. The endocytosis uptake is followed by progressive intracellular accumulation, especially in the perinuclear region, after a few weeks, with no signs of cytotoxicity. Figure 3 demonstrates the desired biocompatibility of the gold metal-coated collagen substrate with the stem cells, showing the internalization of the substrate's component GCNF inside the cells. The process of endocytosis is particularly important for several medical applications, such as drug and gene delivery, particle tracking, and metabolic characterization or achieving organ-specific localization.[41] We foresee that the GCNF materials could act as excellent delivery vehicles for the delivery of growth factors or drug molecules inside the cells.

To assess the biocompatibility of adult stem cells with various substrates, we used the MTT assay and FDA fluorometric technique. Chorion-derived MSCs (Ch-MSC) were cultivated on substrates under different conditions: (1) with complete stem cell medium that maintains the cells in the undifferentiated state; (2) cells exposed to neuronal differentiation medium; and (3) cells treated with one dose of 5AZA for 24 h. The results of the MTT viability and proliferation test are presented in Figure 4.

When no differentiation medium was used, one-way ANOVA analysis (set at $p < 0.05$.) showed a statistically significant increase in proliferation for cells cultivated on collagen and gold-coated collagen (MC) substrate, compared to the control without substrate (Figure 4A). When cells were cultivated for neuronal differentiation, a more sustained statistically significant proliferation resulted in the case of collagen (Figure 4B). We note that the progressive decrease in cell number in the case of gold metal-coated collagen (MC) suggests the initiation of the differentiation process. No significant differences were observed in the case of myocardial differentiation (Figure 4C).

We also performed a cell viability analysis using a two-way ANOVA Bonferroni post-test comparison of grouped data in relationship to the substrates and differentiation media (statistical significance was set at $p < 0.05$). We observed no significant difference between samples (Figure 4D) in all three conditions of cultivation (1, with complete stem cell medium that maintains the cells in undifferentiated state; 2, cells exposed to neuronal differentiation medium; and 3, cells treated with one dose of 5AZA for 24 h).

Ch-MSCs' growth and proliferation were also tested using the fluorescein diacetate (FDA) method. One-way ANOVA analysis (set at $p < 0.05$) showed a significant increase in cellular proliferation when cultivated on the MC substrate and with regular medium. The differentiation conditions resulted in a decrease in cell number when cultivated on the gold-coated collagen coating (MC) (neuronal differentiation *vs* undifferentiated cells, 36.43%; cardiac differentiation *vs* undifferentiated cells, 36.13%; Figure 5A–C). This decrease can be explained by the apoptosis process induced by the differentiation protocols. Differentiation is a process that changes cell size, shape, and metabolic activity due to the complex modifications in gene expression. To begin differentiation, stem cells need signals from the extracellular microenvironment such as growth factors or physicochemical stimuli provided by ECM molecules.

The two-way ANOVA analysis (statistical significance was set at $p < 0.05$) of the FDA analysis for the Ch-MSCs' proliferation in relation to the substrate and differentiation protocols revealed a lower number of cells in the control population or grown on collagen only. One explanation for this behavior could be the proteolytic activity of trypsin on cells at the culture passage used; this seemed to affect strongly the Ch-MSCs' viability and attachment. Interestingly, gold metal-coated collagen increased the attachment of cells to the substrate and sustained cell recovery much better than collagen in all conditions of cultivation: stem cell medium, neuronal differentiation medium, and myocardial differentiation medium.

Differentiation processes such as senescence are modulated by the mitochondrial/oxidative stress pathways; for instance, the successful differentiation of embryonic stem cells requires activation of mitochondrial aerobic metabolism.[42,43] Recent studies have demonstrated that undifferentiated, pluripotent stem cells display lower levels of mitochondrial mass and oxidative phosphorylation and instead preferentially use non-oxidative glycolysis as a primary source of energy.[44] These studies suggest that mitochondrial activity represents an important regulatory mechanism that helps direct stem cell fate. This regulatory role of mitochondria is achieved through the controlled

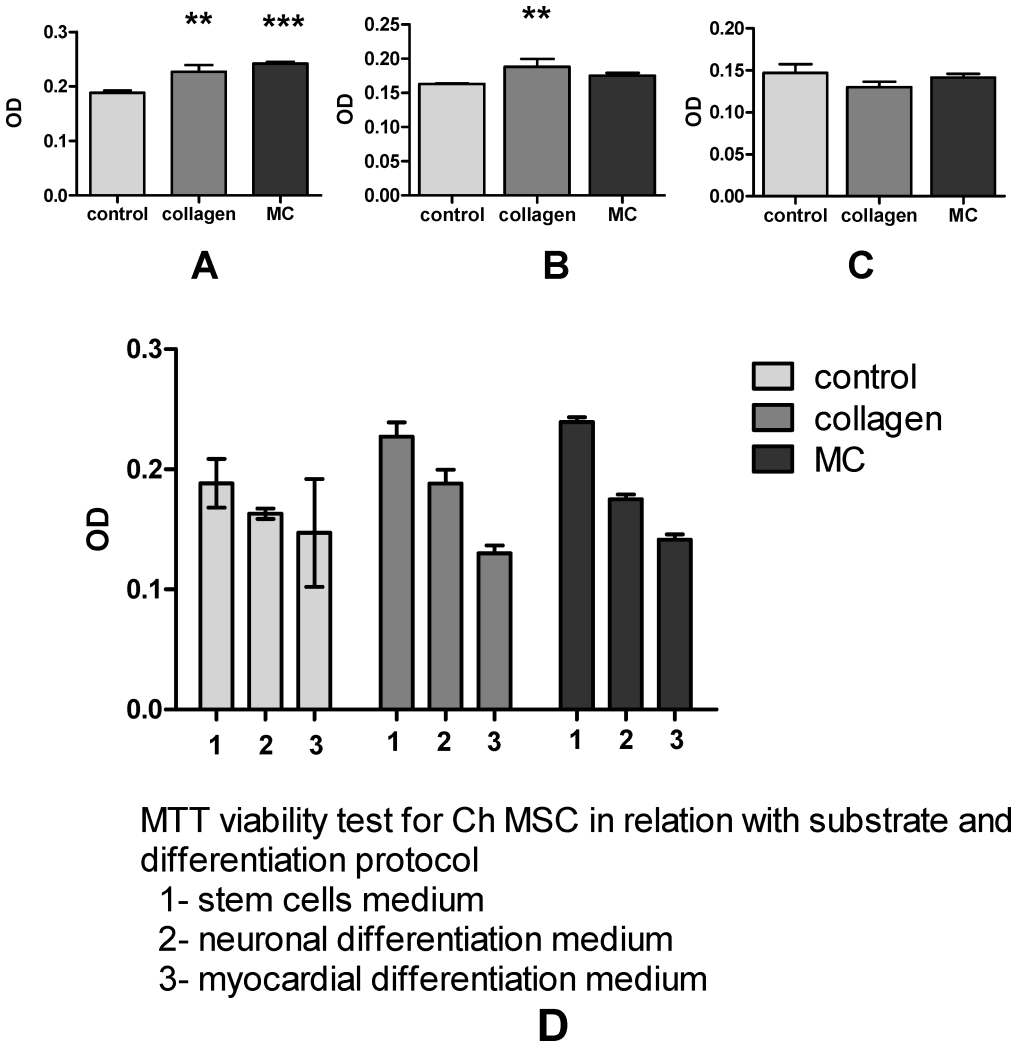

Figure 4. MTT proliferation assay for Ch-MSCs cultivated for 7 days in undifferentiated state (control) (A), in the presence of neuronal differentiation medium (B) and in the presence of myocardial differentiation medium (C), without substrate as control in comparison with substrates: collagen (Coll) and gold-coated collagen (MC). One-way ANOVA analysis showed statistical significance between control *vs* collagen substrate and control *vs* MC (statistical significance was set at $p < 0.05$). Comparing the behavior (viability and proliferation) of Ch-MSC tested with MTT assay, in relation with the substrate and differentiation protocol applied with two-way ANOVA Bonferroni post-test, we observed that there are no statistically significant differences between control *vs* collagen and MC substrates (D).

release of multiple signaling molecules, including reactive oxygen species (ROS) and calcium.[44] GNPs have been shown to be anti-inflammatory agents owing to their ability to inhibit expression of NF-κB and subsequent inflammatory reactions and resistance to oxidation. As a consequence, GNPs have been used in the treatment of diseases such as chronic inflammation, pathological neo-vascularization, rheumatoid arthritis, and neoplastic disorders.[45] The recovery of Ch-MSCs cultivated on gold metal-coated collagen can be explained by the antioxidant and anti-inflammatory activity of the GCNF.

The source of interest in methods that induce differentiation *in vitro* includes the safety advantages of differentiating stem cells in a controlled environment before transplantation, as well as preselection of partially differentiated cells with optimal potential for integration.[46] Therefore, placental-derived MSCs at 5−7 culture passage were used to assess neuronal differentiation. The cells were cultivated on Petri dishes coated with collagen and gold-coated collagen MC in the presence of EGF, bFGF, B27, and N2 supplement for 48 h, with a subsequent exposure for 4 weeks to retinoic acid, IBMX, B27, and N2 supplements. Cells cultivated without substrate were used as controls. The differentiation process was accelerated, and the cells developed more characteristic morphologic features for neuronal lineage in the presence of gold-coated collagen substrates, MC (Figure 6). Placental MSCs grown on MC substrates responded in 1−2 days to neuronal induction medium by generating cells bearing neuronal-like extensions (Figure 6C,D) and neuronal-like morphologies when compared with cells cultivated without substrate (control) (Figure 6A,B).

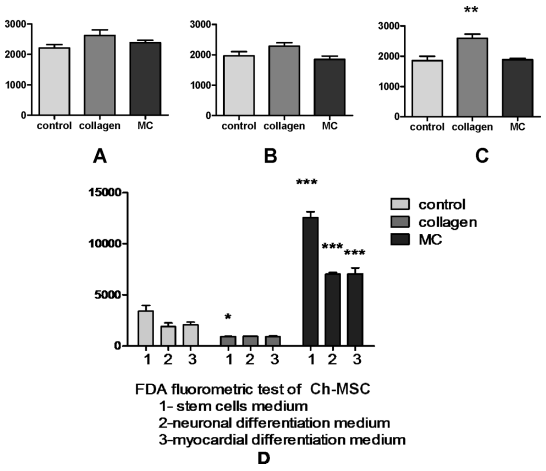

Figure 5. FDA fluorometric test of Ch-MSC cultivated for 7 days in undifferentiated state (control group) (A), in the presence of neuronal differentiation medium (B), and myocardial differentiation medium (C). Each 96-well plate was prepared as follows: control (without substrate), collagen (Coll), and gold metal-coated collagen (MC). The one-way ANOVA analysis of FDA results of proliferation of Ch-MSCs in relation to the type of substrate and differentiation protocols shows a significant increase in cell proliferation in samples cultivated on MC with stem cell medium. Two-way ANOVA comparison Bonferroni post-test of grouped FDA data in relationship with the substrates and differentiation protocol applied of Ch-MSC shows statistically significant differences between substrates: control (without substrate), collagen, and MC (D).

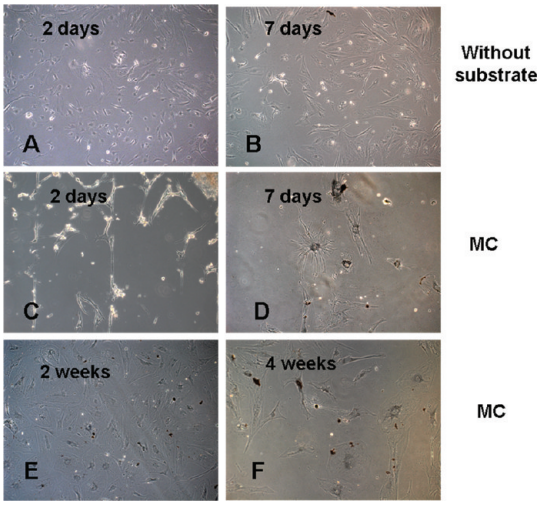

Figure 6. Phase contrast images of chorion-derived MSCs cultivated with neuronal differentiation medium after 2 and 7 days, 2 weeks and 4 weeks (phase contrast 100×). (A,B) Top panel: control cells cultivated without substrate (control). (C–F) Middle and bottom panels: MSC cells cultivated on GCNG substrates, MC. Bars are 100 μm.

Ch-MSCs cultivated on MC substrates formed of GCNF had a characteristic morphology represented by intracellular uptake of gold-adsorbed collagen with an increased level at 2 and 4 weeks (Figure 6E,F).

To assess neuronal differentiation of placental-derived MSCs, we performed immunohystochemical staining of the samples (Figure 7). We observed the expression of GFAP and neurofilament (NF) differentiation markers: GFAP was expressed in cells cultivated without substrate (Figure 7C) and on all substrates used (collagen, gold metal-coated collagen) (Figure 7F,I). Expression of neurofilament (NF) was also observed in differentiated cells on all substrates (collagen and MC), with a greater staining for some cells with a neural-like morphology (Figure 7B,E,H). Additionally, GCNF substrates induced dramatic changes in cell morphology with a strong expression of NF (Figure 7H), with accumulation of GNPs in the perinuclear spaces and in neural-like extensions. Moreover, characteristic alignment of cells was observed for those cultivated on collagen and gold metal-absorbed collagen, suggesting that the presence of collagen-induced orientation of the cells in the same direction (Figure 7A,D,G)

It seems that the combination of gold nanoparticles with collagen is also the most favorable substrate for a more advanced differentiated state of placental MSCs in this experiment. There are some *in vitro* studies regarding neuronal differentiation, neuronal migration, and expansion in the presence of components of ECM such as collagen, fibronectin, laminin, or matrigel.[47–49] Laminin matrices enhanced neuronal stem/progenitor cell migration, expansion, and differentiation into neurons and astrocytes, as well as the elongation of neurites from neuronal stem/progenitor cell-derived neurons.[47] The favorable influence of biochemical and topographical extracellular components on neuritogenesis, neuronal polarity formation, and maturation of axons and dendrites was reported by Gertz *et al.* in a study about the effects of polylactic acid (PLLA) electrospun fiber topography on primary motor neuron development.[48] An advantage of the nanoparticles' presence in combination with ECM proteins as a substrate could be important for regenerative medicine. Kotov *et al.* presented the ability of nanostructures to translocate across the brain–blood barrier; once in the central nervous system, they can migrate along axons and dendrites, suggesting the potential use of nanoparticles as neuronal interfaces for neuronal stimulation in a variety of common or severe neurological diseases.[49]

Another aim of this study was to investigate the cardiomyogenic potential of placental-derived MSCs *in vitro* using different substrates: collagen and GCNFs. The controls were cultivated without substrate. To induce cardiomyogenic differentiation, cells were cultivated in standard stem cell medium for 4 weeks and treated with the demethylating agent 5-azacytidine (10 μM) for 24 h with 1 cycle of exposure/week (in total, 4 cycles of 5AZA). The cardiac phenotype was assessed by immunostaining (Figure 8A–F) with cardiac marker expression after 4 weeks of myocardial differentiation induction: early cardiac specific homeobox protein Nkx 2.5, atrial natriuretic peptide cardiac hormone (ANP),

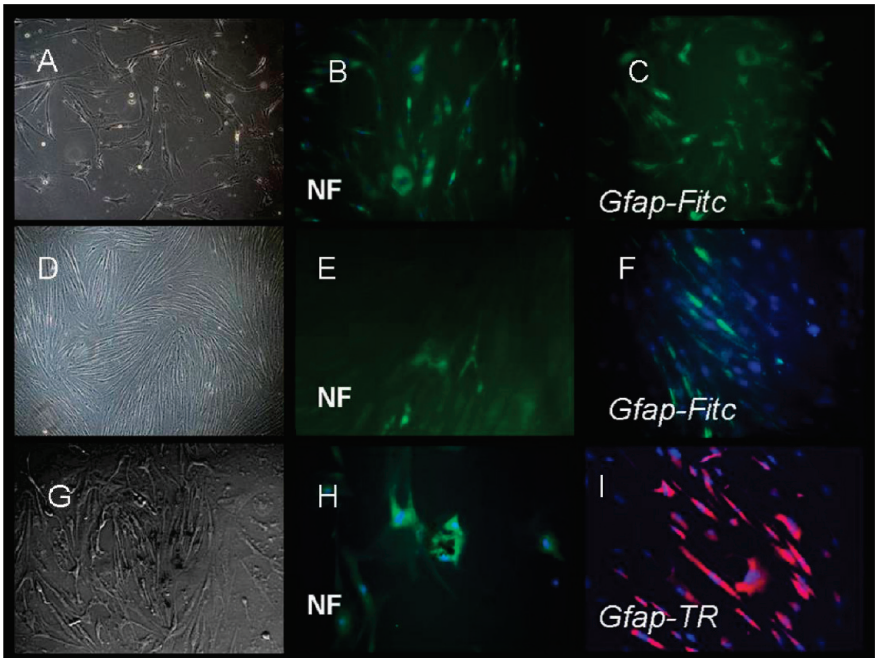

Figure 7. Placental-derived MSC cultivated in neuronal differentiation medium. Top panels: control without substrate. Middle panels: collagen substrate. Bottom panels: gold metal-absorbed collagen substrate. (A) Control without substrate of chorion-derived MSCs cultivated with neuronal differentiation medium for 18 days (phase contrast 100×). (B) Immunostaining for NF-FITC of Ch-MSC without substrate (counterstaining with DAPI) after 4 weeks with neuronal differentiation medium (immunofluorescence, 200× magnification). (C) Immunostaining for GFAP-FITC of chorion-derived MSCs cultivated without substrate of Ch-MSC after 4 weeks of exposure to neuronal differentiation medium (immunofluorescence, 200× magnification). (D) Phase contrast image of Ch-derived MSC cells cultivated on collagen substrate (phase contrast 100×). (E) Immunofluorescence image of Ch-MSC cells cultivated on collagen substrate stained for NF-FITC (200× magnification). (F) Immunostaining for GFAP-FITC of Ch-MSC cultivated on collagen substrate (counterstaining with DAPI, 200× magnification). (G) Chorion-derived MSCs cultivated with neuronal differentiation on MC substrates (phase contrast 200×). (H) Immunostaining for NF-FITC of chorion-derived MSCs cultivated on MC substrates; perinuclear gold metal particles accumulation (immunofluorescence 400×, counterstaining with DAPI). (I) GFAP-TR staining of Ch-MSC cells grown on MC substrate (immunofluorescence 200×, counterstaining with DAPI).

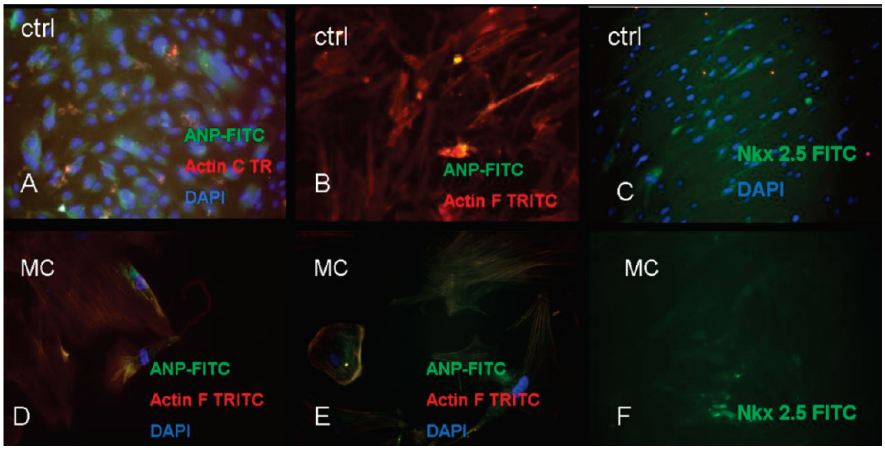

Figure 8. Placental-derived MSCs cultivated in myocardial differentiation medium. (A) Immunostaining for cardiomyocyte markers (ANP-FITC+actin C-TR+DAPI) of Ch-MSC control samples without substrate: cultivated without substrate, 31 days (immunofluorescence, 200× magnification). (B) ANP-FITC and TRITC phalloidin staining of control Ch-MSC cultivated without substrate (immunofluorescence, 200× magnification). (C) Nkx 2.5 FITC expression of Ch-MSC without substrate (immunofluorescence, 100× magnification). (D) ANP-FITC and TRITC phalloidin staining of Ch-MSC cultivated 31 days on MC (immunofluorescence, 400× magnification). (E) ANP-FITC and TRITC phalloidin staining of chorion-derived MSCs cultivated on MC for 31 days (immunofluorescence, 400× magnification). (F) Nkx 2.5 FITC expression of chorion-derived MSCs cultivated 4 weeks on GCNF substrate MC (immunofluorescence, 100× magnification).

and with phalloidin for the rearrangement of filamentous actin (actin F). Ch-MSC adopted a ball-like or polygonal morphology—a morphology consistent with myotube-forming cells as reported by Martin-Rendon *et al.*[50]

This cellular morphology could be explained by the remodeling and assembly of the myofibrils when cells are exposed to an actin-induced stress resulting in the change from a fiber-like to a polygonal shape, morphological aspects more clearly observed in Figure 8D,E.[51]

Immunohistochemical analysis revealed that induced cells were positive for Nkx 2.5 even in the absence of a substrate (Figure 8C). The characteristic stick-like morphology of cells cultivated without substrate was observed after actin-F phalloidin staining (Figure 8B,C). The cardiogenic homeodomain factor Nkx 2.5 cooperates with GATA-4, expressed in early cardiac progenitor cells, to activate the α cardiac actin.[52] Cultivation of Ch-MSCs in the presence of gold metal-absorbed collagen shows the intranuclear localization of Nkx 2.5 (Figure 8F).

Myocardial-induced cells cultivated on gold metal-absorbed collagen were strongly positive for ANP expression in comparison with control cells, despite a shorter cultivation period of 3 weeks (Figure 9A,B).

The effect of 5-azacytidine may not be specific because it induces uncontrolled myogenic speciation and changes in phenotype by activating a large number of genes. Moreover, isolated treatment with 5-azacytidine may not be sufficient to reprogram MSCs to give rise to enough cardiomyocytes for cardiac repair.[51] Other strategies, such as the development of constructs that show both mechanical stimulation in addition to biochemical and electrical stimuli, may be necessary to obtain a fully functional, differentiated cardiac phenotype. GCNF substrates attain all three of these characteristics.

Additionally, we exposed placental-derived MSCs to electrical stimulation, provided by a clinically used pacemaker, with concomitant treatment of cells with neuronal and cardiomyocyte differentiation induction media. Electrical stimulation with the neuronal differentiation protocol accelerated the acquisition of neural-like morphology (Figure 10) even after 24 h of electrical stimulation, and the cells were largely oriented in the same direction after 2 days (Figure 11A,B). Recently, it has also been reported that a greater neuronal cellular extension was induced after the exposure of PC12 cells cultivated on biocompatible carbon nanotube collagen composites to electrical stimulation, facilitating their differentiation into neurons.[53]

Placental MSCs exposed to an electrical field displayed rapid morphological changes and expressed

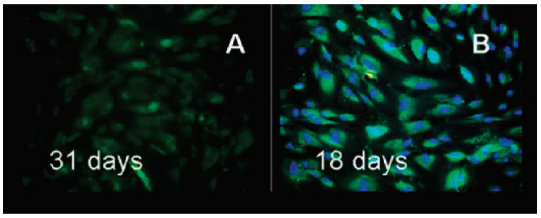

Figure 9. ANP expression of placental-derived MSCs cultivated in myocardial differentiation medium. (A) Immunochemical staining for ANP-FITC of chorion MSCs cultivated without substrate, 31days. (B) Chorion MSCs cultivated on gold metal-absorbed collagen substrate (MC) 18 days after three exposures of 5-azacytidine.

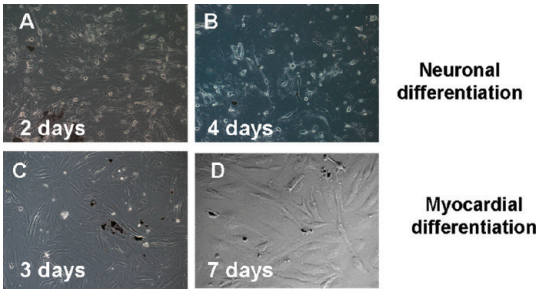

Figure 11. Phase contrast images of neuronal (top panel) and myocardial (bottom panel) induced cells cultivated on metal-absorbed collagen substrates (MC) and exposed to electrical stimulation: (A,B) Ch-MSC after 2 days (A) and 4 days (B) of electrical stimulation (magnification 100×); (C,D) Ch-MSC after 3 days (A, magnification 100×) and 7 days (B, magnification 200×).

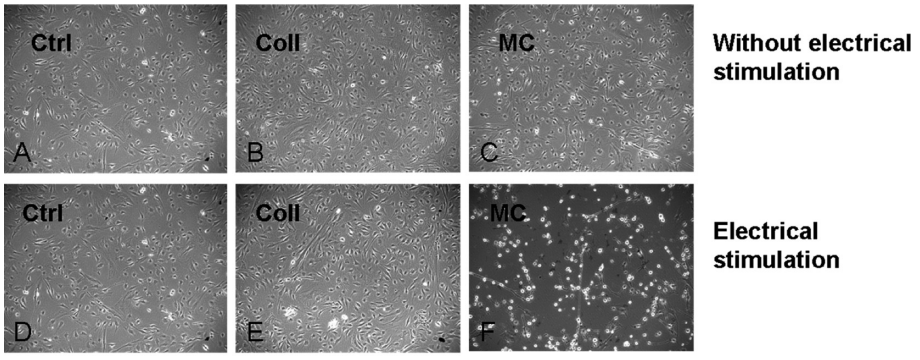

Figure 10. Phase contrast images of neuronal differentiation after 24 h, chorion- derived MSC cells exposed to N1 differentiation medium, without electrostimulation. (Top panels) No electrical stimulation: (A) control without substrate, (B) collagen substrate, (C) gold metal-absorbed collagen. (Bottom panels) With electrical stimulation (D) without substrate, (E) collagen substrate, (F) gold-coated collagen, MC. Bar length represents 200 μm.

cardiac specific genes (troponin I, Nkx 2.5, and GATA-4 analyzed by reverse transcription PCR; data not shown here (Figure 11C,D). The development of a mixed approach to cardiac differentiation—a substrate construct and electrical stimulation—is somewhat common, and most reports show improved cardiac tissue morphology, contractile function, and molecular marker expression when compared with nonstimulated cultures. Hence, electrical stimulation seems to induce at least a similar degree of cardiac myocyte differentiation as mechanical stimulation.[54−56] There are several potential advantages to using collagen-based GNP nanofibers: *in vitro*, predifferentiated mesenchymal stem cells on metal-absorbed collagen substrates can be used for delivery of biologically active molecules, drugs, or genes for *in vivo* transplantation of stem cells in regenerative medicine.

CONCLUSIONS

Collagen-based nanoparticles of various lengths were prepared by reducing $HAuCl_4$ with sodium citrate/$NaBH_4$ and with no reducing agent and by varying the pH conditions. We observed that the optimum pH to obtain short fibers is 3.5. For medium to long fibers having homogeneous sedimentation, the optimum pH was found to be between 5.5 and 6.5. Also, the nanofibers formed with different reduction agents or without any reduction have almost the same length, but they differ in diameter, indicating a non-uniform coverage with gold. Their morphological, optical, and conductive properties were measured by TEM, UV−vis, FTIR, and *I*−*V*. UV−vis spectroscopy showed that the particles' reduction occurs over time and that they did not agglomerate when a reducing agent was used. FTIR confirmed the formation of the metal-absorbed fibers, GCNF. During adsorption of gold nanoparticles on the collagen surface, several interactions—such as electrostatic attraction, covalent bonding, hydrogen bonding—can occur. The adsorption rate is higher in the acidic regions (pH 3.0−6.0) and lower in the alkaline regions (pH 7.0−11), as can be seen from the TEM images. For the chorion placental-derived MSCs, GCNFs have been demonstrated to possess excellent biocompatibility and to improve their neuronal and cardiac differentiation. This combination of biocompatible components of extracellular matrix with gold nanoparticles as delivery systems for drugs, genes, or biologically active molecules can offer solutions for complex problems by *in vivo* transplantation of stem cells for tissue repair and regeneration. The electrically conductive gold metal-coated collagen nanofibers can be further exploited for a more accelerated differentiation process and stimulation of the mesenchymal stem cells.

MATERIALS AND METHODS

Purified bovine Achilles tendon type IV collagen and phosphate buffer solution (PBS pH 7.4) were purchased from Aldrich (Sigma-Aldrich Inc.). Sodium citrate ($C_6H_5O_7Na_3 \cdot 2H_2O$), sodium borohydride ($NaBH_4$), and tetrachloroauric acid ($HAuCl_4 \cdot 3H_2O$) were purchased from Fluka (Sigma-Aldrich Inc.). Soluble collagen was obtained as previously described.[57] $HAuCl_4$ and sodium citrate solutions were prepared in concentrations of 0.1 M. All chemicals were of reagent grade or higher and were used as received unless otherwise specified.

Method Used To Form Gold-Coated Collagen Nanofiber (GCNF) Films. Collagen-based gold nanoparticles were assembled in a novel manner. We modified and adapted the method proposed by Jin *et al.*[58] for the preparation of gold nanoparticles. We used two methods for obtaining metal-absorbed collagen nanofibers: in the presence and absence of reducing agents. Collagen (0.25 g) was dissolved in 0.1 M acetic acid (10 mL) by continuous stirring for 24 h. Reduction agent (sodium citrate or sodium borohydrate) (0.1 M) and $HAuCl_4$ (2.9×10^{-3} M) solutions were prepared separately in 10 and 100 mL of deionized water, respectively. Collagen (1.5 mL) and $HAuCl_4$ (1 mL) solutions were vigorouly mixed together for 10 min in 100 mL of deionized water at different pH ranges (3.5−11) using NaOH (1%). Afterward, 1 mL of reducing agent (0.1 M solution) was added, and the mixture was agitated for 30 min. The product was twice centrifuged at 15 000 rpm for 15 min and washed with double-distilled water. The metal-absorbed nanofibers were analyzed by spectroscopic, microscopic, and conductivity methods. The GCNF-containing solution was deposited onto various substrates and allowed to dry naturally. This step was repeated several times until 20−30 μm thick films were obtained. We have observed a good integration of the layers due to the interactions between the fibrous nanomaterials and their surface charges. One observation was related to the excellent gold−collagen interactions. The GCNFs have been maintained in solutions for over 2 years at room temperature; no Au was observed to bleach, and no changes in the morphological properties of the fibers occurred. This was found to be an extremely stable attachment.

Analytical Characterization. The optical properties of collagen−gold nanowires were monitored using a UV−vis spectrophotometer (JASCO V-570). The morphology of collagen fibers was investigated by TEM in conventional electron beam conditions. Droplets of a 30 μL suspension were pipetted on copper grids (3 mm diameter, 300 meshes) previously covered with parlodion and carbon films. After 2 min, the liquid was absorbed with filter paper. The examination of grids was performed on a JEOL JEM 1010 transmission electron microscope (JEOL, Tokyo, Japan). The images were captured using a Mega VIEW III camera (Olympus, Soft Imaging System, Münster, Germany) and introduced into a database using Soft Imaging System software (Soft Imaging System, Münster, Germany). The diameter of the nanoparticles was analyzed using CellD software (Olympus Soft Imaging Solutions GMBH, Münster, Germany). FTIR measurements were performed with a JASCO 6100 spectrometer in the 4000 to 500 cm^{-1} spectral region with a resolution of 4 cm^{-1} using the KBr pellet technique. Conductivity measurements were performed with a Janis VPF cryostat working in 300−700 K, and resistivity measurements were made using a Keithley instrument. Statistical analyses (mean value, standard deviation, and Student test) were performed using Microsoft Office Excel software (Microsoft Corporation, Redmond, USA).

Cell Cultures. Adult stem cells were isolated from human placenta according to the approved protocols of the Department of Tumor Biology and Radiobiology "Ion Chiricuță" Comprehensive Cancer Center, Cluj Napoca, Romania. Term

placentas from pregnancies with a normal evolution were taken after obtaining the informed consent of the female patients. Briefly, after the amniotic membrane was mechanically separated from the subjacent chorion, the membrane fragment was submitted to an enzymatic digestion treatment in two stages: (1) 0.25% trypsin (Sigma) at 37 °C for 5 min in order to remove epithelial amniotic cells; (2) treatment with 0.25% trypsin + 0.1% collagenase IV (Gibco) for 5 min at 37 °C, followed by inactivation with fetal serum. The chorionic component was also processed mechanically and exposed for 30 min to enzymatic digestion with Dispase (250 μg/mL PBS) (Sigma) + 0.1% collagenase IV (Sigma). Then, the cell suspensions were filtered, and the cells were seeded in culture medium and incubated at 37 °C in 7% CO_2 atmosphere. The MSC culture complete medium was DMEM high glucose/F12-HAM (1:1 ratio), 15% fetal calf serum, 1% antibiotics, 2 mM glutamine, 1% nonessential amino acids, 55 μM β-mercaptoethanol, and 1 mM sodium pyruvate. Isolated and propagated adherent cells had been characterized in a previous study for antigen and gene expression for pluripotency: alkaline phosphatase, Oct-3/4, SOX-2, Nanog, Rex-1, CD29, and CD105.[59]

Differentiation Protocols. Placental-derived mesenchymal stem cells were used after 5−7 passages in standard conditions of cultivation. A collagen-based gold nanofiber substrate was designed by coating the surface of 60 mm culture Petri dishes and 1-well chamber slides using a layer-by-layer system: 1 mL of 15 μg/mL collagen and gold metal-absorbed collagen (MC) solution in PBS was added to 60 mm Petri dishes. After 2−5 min, the solution was discarded, and the plates were allowed to dry in the hood to form an adhesive layer. Another 1 mL of solution was added as previously described, repeating the same procedure three times. For coating 1-well chamber slides, we applied the same layer-by-layer system, and we used 300 μL of collagen and collagen-based gold nanofiber solutions per well. Finally, the plates were allowed to dry and were sterilized by ethylene oxide. After 1−2 h of incubation at 37 °C, the plates were washed three times with PBS and used for cell culture. Control dishes without substrate and with collagen substrate were used. The neuronal differentiation protocol consisted of two steps: (1) cultivation for 48 h with differentiation medium 1, DMEM high glucose/F12-HAM (1:1 ratio), 10% fetal calf serum, 1% antibiotics, 2 mM glutamine, 1% nonessential amino acids, supplemented with 10 ng/mL epidermal growth factor (EGF), 10 ng/mL basic fibroblast growth factor (bFGF), and 1× N2 supplement; (2) cells were exposed to differentiation medium 2 for 3−4 weeks, DMEM high glucose/F12-HAM (1:1 ratio), 10% fetal calf serum, 1% antibiotics, 2 mM glutamine, 1% nonessential amino acids, supplemented 1× N2 supplement, 1× B27 supplement, 3 μM all-trans retinoic acid, and 0.5 mM 3-isobutyl-1-methylxanthine (IBMX). (All reagents were purchased from Sigma Aldrich.) For cardiomyocyte differentiation, placental MSCs cultivated at confluence were seeded in substrate-treated dishes in a stem cell complete medium containing 10 μM 5-azacytidine (Sigma-Aldrich). After incubating for 24 h, the cells were washed twice with phosphate-buffered saline (PBS-Sigma-Aldrich), and the medium was changed to complete medium without 5-azacytidine. The medium was changed every 3−4 days, and one exposure to 10 μM 5-azacytidine was conducted weekly. In control samples, MSCs were cultivated without substrate. The cells were cultivated for 4 weeks, with 4 exposures to 5AZA (1 therapy/week). An additional protocol that we used was cultivation of MSC in cardiomyocyte differentiation medium without substrate for 4 weeks with further cultivation on metalized collagen substrate for another 3 weeks.

Immunohistochemistry. Cells were fixed with 4% paraformaldehyde and permeabilized with 0.1% Triton X-100 in PBS for 20 min at room temperature. Nonspecific antibodies were blocked with 10% BSA (bovine serum albumin) in PBS for 20 min at room temperature. For expression of neuron specific markers, primary antibodies diluted at 1:500 ratio were used for identification of neurofilaments (NF), glial fibrillar acidic protein (GFAP), and CD133 (rabbit antihuman IgG1 Sigma). For identification of cardiomyocyte differentiation markers, the antibodies used were diluted 1:50 in 0.1% BSA in PBS/atrial natriuretic peptide (ANP), cardiac specific homeobox protein Nkx 2.5, and actin (C-2) (all mouse antihuman IgG1, Santa Cruz Biotechnologies). The secondary goat antimouse and goat anti-rabbit antibodies IgG1 were marked with FITC and Texas Red (Santa Cruz Biotechnologies). Incubation with the primary antibody was performed at 4 °C overnight, and, in the case of the secondary antibody, for 45−60 min at 37 °C. TRITC phalloidin from Sigma was used (1:500 in PBS) for staining of filamentous actin. The samples were exposed to an antifade medium containing 4,6-diamidino-2-phenylindole (DAPI) in order to observe nuclei and were examined using an inverted phase Zeiss Axiovert microscope, equipped with soft image analysis Axiovision Rel 4.6, filters 488, 546, and 340/360 nm. Image acquisition was performed with an AxioCam MRC camera.

Proliferation Assay. For assessing substrate biocompatibility, 2×10^4 Ch-MSCs were seeded in a 96-well plate prepared without substrate as control and with substrates—collagen and metallized collagen as described above—and incubated for 7 days with MSC culture complete media. A similar design was created for neuronal and cardiac differentiation using the differentiation protocol described. After incubation, the cells were treated with 0.1% MTT (3-(4,5-dimethylthiazol-2-yl)-2,5-diphenyltetrazolium bromide) and incubated for 1 h for dye incorporation. Blue formazans were eluted in DMSO, and absorbance of the MTT was quantified at 492 nm using a BioTek Synergy 2 fluorescence microplate reader (Winooski, VT, USA). All experiments were performed in triplicate.

Fluorescein Diacetate (FDA) Fluorometric Technique. The 96-well plates were prepared in the same way as described in the proliferation MTT assay, seeded with Ch-MSC, and incubated for 7 days with MSC for control, cardiac, and neuronal differentiation. For the growth and proliferation of cells, a commonly used test with fluorescein diacetate (FDA) was used as an indicator of cell viability. FDA freely diffuses into cells and is rapidly esterified once it enters the cell. The viability of the cells is assessed from the hydrolysis product, fluorescein, which cannot escape from living cells. Fluorescent signals are correlated with the number and the size of individual viable cells. Cell monolayers were washed twice with PBS supplemented with Mg^{2+} and Ca^{2+} and stained for 5 min with FDA in the dark, at 37 °C at a final concentration of 2.4 μM. The wells were washed twice with PBS supplemented with Mg^{2+} and Ca^{2+}. Fluorescence intensity (FI) was measured at 488 nm using a BioTek Synergy 2 fluorescence microplate reader. All experiments were performed in triplicate.

Electrostimulation of Placental-Derived MSC. The collagen-based gold nanoparticle substrates were prepared by coating the surface of 100 mm culture Petri dishes for cardiac differentiation protocol or 60 mm culture Petri dishes for neuronal differentiation, allowed to dry, and equipped with electrodes placed along opposite sides of each dish. The Petri dishes were sterilized by ethylene oxide. Chorion-derived MSCs were seeded in stem cell complete medium, and after they reached near confluence, cardiac and neuronal differentiation protocols were applied with concomitant electrostimulation. For all of the studies, a graphite electrode was used. The electrode lids were connected to a human pacemaker for clinical use (obtained from Cardiovascular and Thoracic Surgery Clinics, Cluj-Napoca) that had been programmed to give 7.5 V pulses (corresponding to 4.5 V/cm) for 1.5 ms at 1 Hz—a range resembling the level required for exciting a normal ventricular tissue. The plates were then incubated at 37 °C in 7% CO_2 atmosphere for 1 week. The setup photo is provided in Figure 3 in the Supporting Information.

Statistical Analysis. Data were analyzed using GraphPad Prism 5 statistics program (La Jolla, CA, USA). We compared the control group with each substrate group using one-way ANOVA Dunnett's Multiple Comparison Test and two-way ANOVA Bonferroni post-test (statistical significance was set at $p < 0.05$).

Acknowledgment. This work was partially suported by the *Investing in people!* PhD scholarship project co-financed by the Sectoral Operational Programme Human Resources Development 2007−2013 Priority Axis 1 "Education and training in support for growth and development of a knowledge based

society" Key area of intervention 1.5: Doctoral and postdoctoral programs in support of research. Contract POSDRU 6/1.5/S/3, "Doctoral Studies: Through Science Towards Society" Babeş-Bolyai University, Cluj-Napoca, Romania. This study was also partially supported by research Grant No. 41−077/2007, titled *Placental stem cells, an alternative source for cell therapy*, Partnership Program 2007, "Iuliu Haţieganu," University of Medicine and Pharmacy, Cluj-Napoca, Romania. A.S.B. and D.C. acknowledge the financial support from the Arkansas Science and Technology Authority and from the U.S. Army, Telemedicine & Advanced Technology Research Center (TATRC).

Supporting Information Available: Additional figures as described in the text. This material is available free of charge *via* the Internet at http://pubs.acs.org.

REFERENCES AND NOTES

1. Romo-Herrera, A. JJ.; Terrones, M.; Terrones, H.; Dag, S.; Meunier, V. Covalent 2D and 3D Networks from 1D Nanostructures: Designing New Materials. *Nano Lett.* **2007**, *7*, 570–576.
2. Solanki, A.; Kim, J. D.; Lee, K. Nanomaterials for Stem Cell Imaging: Nanoparticle-Based Applications for Regenerative Medicine. *Nanomedicine* **2008**, *3*, 567–578.
3. Guo, S. Z.; Zhang, C.; Wang, W. Z.; Liu, T. X. Preparation and Characterization of Organic−Inorganic Hybrid Nanomaterials Using Polyurethane-*b*-Poly[3-(trimethoxysilyl) Propyl Methacrylate *via* RAFT. *Polym. Lett.* **2010**, *4*, 17–25.
4. Sayari, A.; Hamoudi, S. Periodic Mesoporous Silica Based Organic−Inorganic Nanocomposite Materials. *Chem. Mater.* **2001**, *13*, 3151–3168.
5. Abed, O.; Wanunu, M.; Vaskevich, A.; Arad-Yellin, R.; Shanzer, A.; Rubinstein, I. Reversible Binding of Gold Nanoparticles to Polymeric Solid Supports. *Chem. Mater.* **2006**, *18*, 1247–1260.
6. Braun, E.; Eichen, Y.; Sivan, U.; Ben-Yoseph, G. DNA-Template Assembly and Electrode Attachment of a Conducting Silver Wire. *Nature* **1998**, *391*, 775–778.
7. Lee, S. W.; Mao, C. B.; Flynn, C. E.; Belcher, A. M. Ordering of Quantum Dots Using Genetically Engineered Viruses. *Science* **2002**, *296*, 892–895.
8. Papapostolou, D.; Smith, A. M.; Atkins, E. D. T.; Oliver, S. J.; Ryadnov, M. G.; Serpell, L. C.; Woolfson, D. N. Engineering Nanoscale Order into a Designed Protein Fiber. *Proc. Natl. Acad. Sci. U.S.A.* **2007**, *104*, 10853–10858.
9. Yuwono, V. M.; Hartgerink, J. D. Peptide Amphiphile Nanofibers Template and Catalyze Silica Nanotube Formation. *Langmuir* **2007**, *23*, 5033–5038.
10. Tamerler, C.; Sarikaya, M. Genetically Designed Peptide-Based Molecular Material. *ACS Nano* **2009**, *3*, 1606–1615.
11. Reches, M.; Gazit, E. Controlled Patterning of Aligned Self-Assembled Peptide Nanotubes. *Nat. Nanotechnol.* **2006**, *1*, 195–200.
12. Woolfson, D. N.; Ryadnov, M. G. Peptide-Based Fibrous Biomaterials: Some Things Old, New and Borrowed. *Curr. Opin. Chem. Biol.* **2006**, *10*, 559–567.
13. Toda, A.; Okabe, M.; Yoshida, T.; Nikaido, T. The Potential of Amniotic Membrane/Amnion-Derived Cells for Regeneration of Various Tissues. *J. Pharmacol. Sci.* **2007**, *105*, 215–228.
14. Liu, Z. J.; Zhuge, Y.; Velazquez, O. C. Trafficking and Differentiation of Mesenchymal Stem Cells. *J. Cell. Biochem.* **2009**, *106*, 984–991.
15. Pittenger, M. F.; Mackay, A. M.; Beck, S. C.; Jaiswal, R. K.; Douglas, R. J.; Mosca, D.; Moorman, M. A.; Simonetti, D. W.; Craig, S.; Marshak, D. R. Multilineage Potential of Adult Human Mesenchymal Stem Cells. *Science* **1999**, *284*, 143–147.
16. Prockop, D. J. Marrow Stromal Cells as Stem Cells for Nonhematopoietic Tissues. *Science* **1997**, *276*, 71–74.
17. Antonitsis, P.; Papagiannaki, E. I.; Kaidoglou, A.; Papakonstantinou, C. *In Vitro* Cardiomyogenic Differentiation of Adult Human Bone Marrow Mesenchymal Stem Cells. The Role of 5-Azacytidine C. *Inter. Cardiovasc. Thorac. Surg.* **2007**, *6*, 593–597.
18. Walther, G.; Gekas, J.; Bertrand, O. F. Amniotic Stem Cells for Cellular Cardiomyoplasty: Promises and Premises. *Cather. Cardiovasc. Interv.* **2009**, *73*, 917–24.
19. Pittenger, M. F.; Martin, B. Mesenchymal Stem Cells and Their Potential as Cardiac Therapeutics. *J. Circ. Res.* **2004**, *95*, 9–20.
20. Zhou, H.; Zhou, J.; Gupta, A.; Zou, T. Derived Carbon for Growth and Differentiation of Neuronal Cells. *Int. J. Mol. Sci.* **2007**, *8*, 884–893.
21. Park, K. H.; Kim, K. H.; Na, K. Neuronal Differentiation of PC12 Cells Cultured on Growth Factor-Loaded Nanoparticles Coated on PLGA Microspheres. *J. Microbiol. Biotechnol.* **2009**, *19*, 1490–1495.
22. Solanki, A.; Kim, J. D.; Lee, K. Nanomaterials for Stem Cell Imaging: Nanoparticle-Based Applications for Regenerative Medicine. *Nanomedicine* **2008**, *3*, 567–578.
23. Zharov, V. P.; Galitovskaya, E. N.; Johnson, C.; Kelly, T. Synergistic Enhancement of Selective Nanophotothermolysis with Gold Nanoclusters: Potential for Cancer Therapy. *Lasers Surg. Med.* **2005**, *37*, 219–226.
24. Castaneda, L.; Valle, J.; Yang, N.; Pluskat, S.; Slowinska, K. Collagen Cross Linking with Au Nanoparticles. *Biomacromolecules* **2008**, *9*, 3383–3388.
25. Mahl, D.; Greulich, C.; Zaika, W. M.; Köller, M.; Epple, M. Gold Nanoparticles: Dispersibility in Biological Media and Cell-Biological Effect. *J. Mater. Chem.* **2010**, *20*, 6176–6181.
26. Flavel, B.; Nussio, M.; Quinton, J.; Shapter, J. Adhesion of Chemically and Electrostatically Bound Gold Nanoparticles to a Self-Assembled Silane Monolayer Investigated by Atomic Force Volume Spectroscopy. *J. Nano. Res.* **2009**, *11*, 2013–2022.
27. Zheng, B.; Qian, L.; Yuan, H.; Xiao, D.; Yang, X.; Paau, M. C.; Choi, M. M. F. Preparation of Gold Nanoparticles on Eggshell Membrane and Their Biosensing Application. *Talanta* **2010**, *82*, 177–183.
28. Harris, R.; Reiber, A. Influence of Saline and pH on Collagen Type I Fibrillogenesis *In Vitro*: Fibril Polymorphism and Colloidal Gold Labellin. *Micron* **2007**, *38*, 513–521.
29. Levy, R.; Thanh, N. T. K.; Doty, R. C.; Hussain, I.; Nichols, R. J.; Schiffrin, D. J.; Brust, M.; Fernig, D. G. Rational and Combinatorial Design of Peptide Capping Ligands for Gold Nanoparticles. *J. Am. Chem. Soc.* **2004**, *126*, 10076–10084.
30. Kim, J. U.; Cha, S. H.; Shin, K.; Jho, J. Y.; Lee, J. C. Preparation of Gold Nanowires and Nanosheets in Bulk Block Copolimer Phases under Mild Conditions. *Adv. Mater.* **2004**, *16*, 456–459.
31. Zhou, M.; Bron, M.; Schuhmann, W. Controlled Synthesis of Gold Nanostructures by a Thermal Approach. *J. Nanosci. Nanotechnol.* **2008**, *8*, 3465–3472.
32. Porter, M. D.; Bright, T. B.; Allara, D. L.; Chidsey, C. E. Spontaneously Organized Molecular Assemblies. 4. Structural Characterization of N-Alkyl Thiol Monolayers on Gold by Optical Ellipsometry, Infrared Spectroscopy, and Electrochemistry. *J. Am. Chem. Soc.* **1987**, *109*, 3559–3568.
33. Orza, A.; Olenic, L.; Pruneanu, S.; Pogacean, F.; Biris, A. S. Morphological and Electrical Characteristics of Amino Acid−AuNP Nanostructured Two-Dimensional Ensembles. *Chem. Phys.* **2010**, *373*, 295–299.
34. Hwang, N. S.; Varghese, S.; Elisseeff, J. Controlled Differentiation of Stem Cells. *Adv. Drug Delivery Rev.* **2008**, *60*, 199–214.
35. Li, Y.; Shipton, M. K.; Ryan, J.; Kaufman, E. D.; Franzen, S.; Feldheim, D. L. Synthesis, Stability, and Cellular Internalization of Gold Nanoparticles Containing Mixed Peptide-Poly(ethylene glycol) Monolayers. *Anal. Chem.* **2007**, *79*, 2221–2229.
36. Chithrani, D. B. Intracellular Uptake, Transport, and Processing of Gold Nanostructures. *Mol. Membr. Biol.* **2010**, *27*, 299–311.
37. Evans, H. J.; Sweet, J. K.; Price, R. L.; Yost, M.; Goodwin, R. L. A Novel 3-D Culture System for the Study of Cardiac Myocyte Development. *Am. J. Phys., Heart Circ. Phys.* **2003**, *285*, 570–578.
38. Rowlands, A. S.; George, P. A.; Cooper-White, J. J. Directing Osteogenic and Myogenic Differentiation of MSCs: Interplay

of Stiffness and Adhesive Ligand Presentation. *Am. J. Phys.: Cell Phys.* **2008**, *295*, C1037–C1044.
39. Suzuki, S.; Narita, Y.; Yamawaki, A.; Murase, Y.; Satake, M.; Mutsuga, M.; Okamoto, H.; Kagami, H.; Ueda, M.; Ueda, Y. Effects of Extracellular Matrix on Differentiation of Human Bone Marrow-Derived Mesenchymal Stem Cells into Smooth Muscle Cell Lineage: Utility for Cardiovascular Tissue Engineering. *Cells Tiss. Org.* **2010**, *191*, 269–280.
40. Lars, H. E.; Signe, I.; Henrik, J. J.; Thore, H.; Daniel, H. M.; Boye, S. N.; Niels, B. The Collagen Receptor uPARAP/Endo180. *Front. Biosci.* **2009**, *14*, 2103–2114.
41. Nagesha, D.; Laevsky, G. S.; Lampton, P.; Banyal, R.; Warner, C.; DiMarzio, C.; Sridhar, S. *In Vitro* Imaging of Embryonic Stem Cells Using Multiphoton Luminescence of Gold Nanoparticles. *Int. J. Nanomed.* **2007**, *2*, 813–819.
42. Facucho-Oliveira, J. M.; John, J. C. The Relationship between Pluripotency and Mitochondrial DNA Proliferation during Early Embryo Development and Embryonic Stem Cell Differentiation. *Stem Cells Rev.* **2009**, *5*, 140–158.
43. Prigione, A.; Fauler, B.; Lurz, R.; Lehrach, H.; Adjaye, J. The Senescence-Related Mitochondrial/Oxidative Stress Pathway Is Repressed in Human Induced Pluripotent Stem Cells. *Stem Cells* **2010**, *28*, 721–733.
44. Rehman, J. Empowering Self-Renewal and Differentiation: The Role of Mitochondria in Stem Cells. *J. Mol. Med.* **2010**, *88*, 981–986.
45. Barathmanikanth, S.; Kalishwarala, K.; Sriram, M.; Pandian, S. R. K.; Youn, H.; Eom, S.; Gurunathan, S. Anti-Oxidant Effect of Gold Nanoparticles Restrains Hyperglycemic Conditions in Diabetic Mice. *J. Nanobiotechnol.* **2010**, *8*, 1–15.
46. MacLaren, R. E.; Pearson, R. A.; MacNeil, A.; Douglas, R. H.; Salt, T. E.; Akimoto, M.; Swaroop, A.; Sowden, J. C.; Ali, R. R. Retinal Repair by Transplantation of Photoreceptor Precursors. *Nature* **2006**, *444*, 203–207.
47. Flanagan, L. A.; Rebaza, L. M.; Derzic, S.; Schwartz, P. H.; Monuki, E. S. Regulation of Human Neural Precursor Cells by Laminin and Integrins. *J. Neurosci. Res.* **2006**, *83*, 845–856.
48. Gertz, C. C.; Leach, M. K.; Birrell, L. K.; Martin, D. C.; Feldman, E. L.; Corey, J. M. Accelerated Neuritogenesis and Maturation of Primary Spinal Motor Neurons in Response to Nanofibers. *Dev. Neurobiol.* **2010**, *70*, 589–603.
49. Kotov, N. A.; Winter, J. O.; Clements, I. P.; Jan, E.; Timko, B. P.; Campidelli, S. T.; Pathak, S.; Mazzatenta, A.; Lieber, Ch. M.; Prato, M.; *et al.* Nanomaterials for Neural Interfaces. *Adv. Mater.* **2009**, *21*, 3970–4004.
50. Rendon, M. E.; Sweeney, D.; Lu, F.; Girdlestone, J.; Navarrete, C.; Watt, S. M. 5-Azacytidine-Treated Human Mesenchymal Stem/Progenitor Cells Derived from Umbilical Cord, Cord Blood and Bone Marrow Do Not Generate Cardiomyocytes *In Vitro* at High Frequencies. *Vox Sang.* **2008**, *95*, 137–148.
51. Boateng, Y S. L.; Goldspink, P. H. Assembly and Maintenance of the Sarcomere Night and Day. *Cardiovasc. Res.* **2008**, *77*, 667–675.
52. Sepulveda, J. L.; Belaguli, N.; Nigam, V.; Chen, C. Y.; Nemer, M.; Schwartz, R. GATA-4 and Nkx-2.5 Coactivate Nkx-2 DNA Binding Targets: Role for Regulating Early Cardiac Gene Expression. *J. Mol. Cell. Biol.* **1998**, *18*, 3405–3415.
53. Cho, Y.; Borgens, R. B. The Effect of an Electrically Conductive Carbon Nanotube/Collagen Composite on Neurite Outgrowth of PC12 Cells. *J. Biomed. Mater. Res.* **2010**, *95*, 510–517.
54. Martherus, R. S.; Volkert, A. Z.; Ayoubi, T. A. Y. Electrical Signals Affect the Cardiomyocyte Transcriptome Independently of Contraction. *Biotechniques* **2010**, *48*, 65–67.
55. Fink, C.; Ergun, S.; Kralisch, D.; Remmers, U.; Weil, J.; Eschenhagen, T. Chronic Stretch of Engineered Heart Tissue Induces Hypertrophy and Functional Improvement. *FASEB J.* **2000**, *14*, 669–679.
56. Zimmermann, W. H.; Schneiderbanger, K.; Schubert, P.; Didie, M.; Munzel, F.; Heubach, J. F.; Kostin, S.; Neuhuber, W. L.; Eschenhagen, T. Tissue Engineering of a Differentiated Cardiac Muscle Construct. *Circ. Res.* **2002**, *90*, 223–230.
57. Hichman, D.; Simes, T. J.; Miles, C. A. Isinglass/Collagen: Denaturation and Functionality. *J. Biotechnol.* **2000**, *79*, 245–257.
58. Jin, Y.; Kang, X.; Song, Y.; Zhang, B.; Cheng, G.; Dong, S. Controlled Nucleation and Growth of Surface-Confined Gold Nanoparticles on a (3-Aminopropyl)trimethoxysilane-Modified Glass Slide: A Strategy for SPR Substrates. *Anal. Chem.* **2001**, *73*, 2843–2849.
59. Mihu, C. M.; Ciuca, D. R.; Soritau, O.; Susman, S.; Mihu, D. Isolation and Characterization of Mesenchymal Stem Cells from the Amniotic Membrane. *Rom. J. Morphol. Embryol.* **2009**, *50*, 73–77.